


Why Moist Dynamic Processes Matter for the Sub-Seasonal Prediction of Atmospheric Blocking Over Europe

Journal Article**Author(s):**

Wandel, Jan; [Büeler, Dominik](#) ; Knippertz, Peter; Quinting, Julian F.; Grams, Christian M.

Publication date:

2024-04-28

Permanent link:

<https://doi.org/10.3929/ethz-b-000669214>

Rights / license:

[Creative Commons Attribution 4.0 International](#)

Originally published in:

Journal of Geophysical Research: Atmospheres 129(8), <https://doi.org/10.1029/2023JD039791>

Why Moist Dynamic Processes Matter for the Sub-Seasonal Prediction of Atmospheric Blocking Over Europe

**Key Points:**

- Warm conveyor belt (WCB) activity around the onset of atmospheric blocking over Europe (EuBL) is analyzed in reanalysis and sub-seasonal reforecasts
- Correct WCB prediction provides a sub-seasonal window of forecast opportunity for EuBL onset
- Synoptic activity over the North Pacific supports the development of a teleconnection that affects EuBL onset

Supporting Information:

Supporting Information may be found in the online version of this article.

Correspondence to:

J. Wandel,
Jan.Wandel@dwd.de

Citation:

Wandel, J., Büeler, D., Knippertz, P., Quinting, J. F., & Grams, C. M. (2024). Why moist dynamic processes matter for the sub-seasonal prediction of atmospheric blocking over Europe. *Journal of Geophysical Research: Atmospheres*, 129, e2023JD039791. <https://doi.org/10.1029/2023JD039791>

Received 12 AUG 2023

Accepted 15 MAR 2024

Jan Wandel^{1,2} , Dominik Büeler^{1,3} , Peter Knippertz¹ , Julian F. Quinting¹ , and Christian M. Grams^{1,4} 

¹Institute of Meteorology and Climate Research Troposphere Research (IMKTRO), Karlsruhe Institute of Technology (KIT), Karlsruhe, Germany, ²Now at Deutscher Wetterdienst, Offenbach, Germany, ³Now at Institute for Atmospheric and Climate Science, ETH Zürich, Zürich, Switzerland, ⁴Now at Federal Office of Meteorology and Climatology, MeteoSwiss, Zurich-Airport, Zürich, Switzerland

Abstract In recent years, there has been growing evidence that latent heat release in midlatitude weather systems such as warm conveyor belts (WCBs) contributes significantly to the onset and maintenance of blocking anticyclones (blocked weather regimes). Still, numerical weather prediction (NWP) and climate models struggle to correctly predict and represent atmospheric blocking in particular over Europe. Here, we elucidate the representation of WCB activity in 20 years of extended winter (1997–2017) of European Centre for Medium-Range Weather Forecast's IFS reforecasts around the onset of blocking over Europe (EuBL) employing different perspectives. First, we show that the model struggles to predict EuBL onsets already at 10–14 days lead time in line with a misrepresentation of WCB activity in the ensemble mean. However, we also find cases with accurate EuBL forecasts even in pentad 4 (15–19 days). This subset of successful forecasts at extended-range lead times goes in line with accurate WCB forecasts over the North Atlantic several days prior to the blocking onset. Second, investigating the time-lagged relationship of blocking onset and WCB activity, we find that WCB activity over the North Atlantic emerges well prior to the onset of the block and that different pathways into EuBL exist in the reforecasts compared to reanalysis. Finally, we find indication of predictability associated with a Rossby wave train emerging from the North Pacific. Although our study can not disentangle the roles of intrinsic predictability limits and model deficiencies, we show that correct predictions of EuBL go along with distinct patterns of WCB activity.

Plain Language Summary Warm conveyor belts (WCBs) are weather systems associated with low pressure systems which occur predominantly over the ocean regions of the midlatitudes. Several recent studies highlight the role of latent heat release due to cloud formation in WCBs for the development of long-lived high pressure systems. However, current weather prediction and climate models struggle to accurately predict these high pressure systems, particularly over Europe (EuBL). This study, based on 20 years (1997–2017) of forecast data, reveals challenges in predicting WCB activity together with the onset of EuBL, especially within a lead time of 10–14 days. Successful predictions at extended lead times (15–19 days) align with precise forecasts of WCB activity over the North Atlantic and North Pacific, indicating a connection between these regions. Examining the timing of the onset of EuBL and WCB activity, we show that WCB activity over the North Atlantic precedes EuBL. Additionally, we identify both correct and incorrect pathways leading to EuBL and suggest that predictability of EuBL may arise from specific atmospheric patterns, particularly related to Rossby waves in the North Pacific.

1. Introduction

Atmospheric blocking describes the formation of persistent, large-scale anticyclonic circulation anomalies that block the westerly flow and eastward propagation of synoptic eddies (Berggren et al., 1949; Rex, 1950). Blocking can be associated with extreme weather events such as flooding in adjacent regions, heat waves or thunderstorm episodes in summer (Mohr et al., 2019; Oertel, Pickl, et al., 2023; Pfahl & Wernli, 2012) and cold spells in winter (Buehler et al., 2011; Ferranti et al., 2018). Thus, the accurate prediction of blocking on sub-seasonal to seasonal (S2S) time scales (more than 10–15 days but less than a season ahead, depending on the definition) is desirable for decision makers to prepare for extreme weather events and to issue early warnings. Early blocking studies developed theories for the formation and maintenance of blocking by planetary waves or orographic forcing (Charney & DeVore, 1979; Hoskins & Karoly, 1981). However, they could not explain some observed

© 2024. The Authors.

This is an open access article under the terms of the [Creative Commons Attribution License](https://creativecommons.org/licenses/by/4.0/), which permits use, distribution and reproduction in any medium, provided the original work is properly cited.

characteristics such as the rapid onset (Nakamura & Huang, 2018) or the fluctuation in size and intensity during the blocking life cycle (Dole, 1986).

These restrictions point to the importance of transient eddies and synoptic-scale processes for the formation and maintenance of atmospheric blocking (Shutts, 1983). Until recently, the evaluation of these processes has almost exclusively been done on the basis of dry dynamics (Colucci, 1985; Yamazaki & Itoh, 2013). However, Pfahl et al. (2015) showed that moist dynamic processes, in particular latent heat release (LHR) due to cloud formation, are of first-order importance for the onset and maintenance of atmospheric blocking. An overview on how midlatitude LHR affects the large-scale circulation is given in various studies (e.g., Grams & Archambault, 2016). Here we briefly summarize the main findings.

Intense LHR occurs in poleward ascending air streams in the warm sector of extratropical cyclones, in so-called warm conveyor belts (WCBs) (Madonna et al., 2014; Wernli, 1997). In a WCB relatively warm and humid air from the lower troposphere starts ascending slantwise along the tilted (moist-)isentropes of a baroclinic zone. Condensation sets in and the associated LHR accelerates vertical motion and facilitates cross-isentropic ascent. This injects an air mass into the upper troposphere resulting in divergent outflow, a lifting of the tropopause, a poleward deflection of the upper-level jet (Grams et al., 2011; Pomroy & Thorpe, 2000) and ultimately the formation of an upper-level ridge. If sustained for a longer time period, the diabatically enhanced outflow can result in the onset of a block (e.g., Grams & Archambault, 2016; Maddison et al., 2019; Riboldi et al., 2019; Steinfeld & Pfahl, 2019). To quantify the effect of diabatically enhanced outflow for the onset and maintenance of blocks, Steinfeld et al. (2020) conducted numerical experiments for various case studies suppressing diabatically enhanced outflow through switching off LHR. Without LHR and its associated divergent outflow blocks were found to be considerably weaker or even absent. Using a quantitative diagnostic framework based on potential vorticity thinking, Teubler and Riemer (2021) and Hauser et al. (2023a, 2023b) confirmed the importance of moist dynamics for the amplification of upper-tropospheric ridges and blocking.

WCBs are challenging to predict due to the small-scale cloud-microphysical processes associated with their air stream (Oertel et al., 2020; Oertel, Miltenberger, et al., 2023) thereby facing both intrinsic limits of predictability and problems in an accurate representation in models. In a previous study, we could show that skillful predictions of WCBs in current numerical weather prediction (NWP) models are possible only until around 8–10 days (Wandel et al., 2021). Despite apparent intrinsic limits of predictability for the WCB, for example, Maddison et al. (2020) showed that there is still room for improvements in the representation of diabatic processes in NWP models which again have the potential to improve the prediction of blocking.

The representation of atmospheric blocking in NWP and climate models has been investigated in numerous studies in the last two decades. Many studies point to the underestimation of blocking frequency (negative bias) over the European region (d'Andrea et al., 1998; Masato et al., 2014). This bias increases with longer lead time (Jia et al., 2014; Quinting & Vitart, 2019) and can be reduced through higher horizontal and vertical resolution (Anstey et al., 2013; Davini et al., 2017; Dawson et al., 2012). Remarkably, comparing the forecast skill for different weather regimes, Büeler et al. (2021) found that the year-round forecast horizon for blocking over the Central European region is 3–5 days shorter compared to other large-scale flow regimes. NWP models particularly struggle predicting the onset of EuBL (Ferranti et al., 2015; Rodwell et al., 2013). These difficulties can partly be linked to its lower intrinsic predictability (Faranda et al., 2016; Hochman et al., 2021), but might also be a result of physical processes, such as LHR in WCBs, which are still difficult for the models to accurately capture (cf. Maddison et al., 2020).

For an individual case study, Grams et al. (2018) highlighted the role of WCBs for the onset of blocking over Europe in one of the most severe forecast busts in the ECMWF's integrated forecasting system (IFS) in the last decade. They find that a misrepresentation of the WCB in the ensemble forecasting system amplified the initial condition error and triggered a nonlinear feedback mechanism. The WCB communicated the forecast error from small scales to the upper troposphere and downstream, which led to the missed onset of the block. Other studies also point to the amplification of errors in the WCBs (Pickl et al., 2023) or highlight the generation of errors in potential temperature and potential vorticity in the WCBs, which can lead to downstream errors in the Rossby wave pattern (Berman & Torn, 2019; Martínez-Alvarado et al., 2016). Moreover, teleconnections from the Caribbean and North Pacific region affect the occurrence of large-scale weather regimes, including blocking, in the European region (Michel & Rivière, 2011; Michel et al., 2012) and the teleconnection itself is again modulated by WCB activity (Quinting et al., 2024).

However, so far a systematic investigation of the role of WCBs for the prediction of atmospheric blocking over Europe is still missing, primarily due to the lack of a diagnostic framework.

Here, we employ different perspectives to investigate, for the first time, the systematic link between WCBs and blocking in ECMWF's IFS S2S reforecasts and reanalysis in the extended winter period from 1997 to 2017. We address the following three research questions:

- What is the link between WCB activity and EuBL onset and how well is it represented in reforecasts at different forecast lead times?
- Is there a link between WCB representation and correct forecasts of EuBL onset?
- Do teleconnections from the North Pacific region play a role for the prediction of EuBL?

We focus on EuBL onsets in different pentads (lead times of 0–4 days, 5–9 days, 10–14 days, and 15–19 days) since forecast skill for Atlantic-European weather regimes and WCBs on average vanishes in week 2 (7–14 days) (Büeler et al., 2021; Osman et al., 2023; Wandel et al., 2021). Onsets of large-scale and persistent flow regimes at lead times of 5–20 days are of particular interest from a sub-seasonal prediction perspective, because, due to their persistence, they strongly influence the circulation even beyond lead times of 20 days.

The data, the definition of EuBL, and the Eulerian metric to identify WCBs are introduced in Section 2. We then elucidate the potential link of WCB activity and EuBL onset from four different angles. (a) In Section 3, we first investigate how well WCB activity around EuBL onset is represented in the ensemble mean of IFS reforecasts at different forecast lead times. (b) Section 4.1 then explores potential causalities between the representation of WCB activity in individual ensemble members and the prediction of EuBL onset. (c) Furthermore, we explore the representation of the time-lagged evolution of WCB activity prior to EuBL onset depending on the ability of the model to predict EuBL onset in Section 4.2. (d) Finally, the role of upstream precursors from the Pacific for the prediction of EuBL is analyzed in Section 5 and the study ends with concluding remarks in Section 6.

2. Data and Method

2.1. Reforecasts and Reanalysis

We use the ECMWF's IFS sub-seasonal ensemble reforecasts (Vitart, 2017) for the extended winter period (NDJFM) from 1997 to 2017 to analyze WCBs and 500-hPa geopotential height (Z500). The ensemble reforecasts contain in total 11 members, of which one member is an unperturbed control forecast. To increase our sample size, we use all reforecasts for IFS cycles CY43R1, CY43R3, and CY45R1, which were operational between 22.11.2016 and 11.6.2019. Reforecasts were computed twice-weekly during that period for the respective calendar day and the last 20 years. This yields a total of 1,641 initialization times in the study period 1997–2017. Consistently with the initial conditions of the reforecasts, we employ ERA-Interim reanalysis data (Dee et al., 2011a) for verification. Both data sets are retrieved on a regular $1.5^\circ \times 1.5^\circ$ latitude–longitude grid and remapped to $1^\circ \times 1^\circ$ grid spacing using linear interpolation. We calibrate the reforecasts by calculating WCB and Z500 anomalies relative to the 90-day running mean model climatology at a given lead time derived from the 20-year reforecast data using all cycles. Anomalies for ERA-Interim are computed against ERA-Interim climatology for 1997–2017. This approach eliminates the systematic bias between ERA-Interim and the reforecasts.

2.2. Atlantic-European Weather Regimes

To identify blocking over the European region, we use seven year-round Atlantic-European weather regimes based on 5-day low-pass-filtered geopotential height (Büeler et al., 2021; Grams et al., 2017). Thus, we refer to atmospheric blocking using the definition of blocked weather regimes. Weather regimes are quasi-stationary, persistent, and recurrent large-scale flow patterns in the midlatitudes (Michelangeli et al., 1995; Vautard, 1990) and reflect the variability of the large-scale extratropical circulation on sub-seasonal timescales. An accurate prediction of large-scale flow regimes is particularly important since it yields more useful information about different surface variables (e.g., temperature and precipitation) after forecast day 10–15 compared to the direct NWP model output (Bloomfield et al., 2021; Mastrantonas et al., 2022). Blocking over the European region (EuBL) is the dominant blocked regime in winter (compared to “Scandinavian Blocking” in summer) and occurs at around 11% of winter days. For the computation of the regime patterns the interested reader is referred to Büeler et al. (2021).

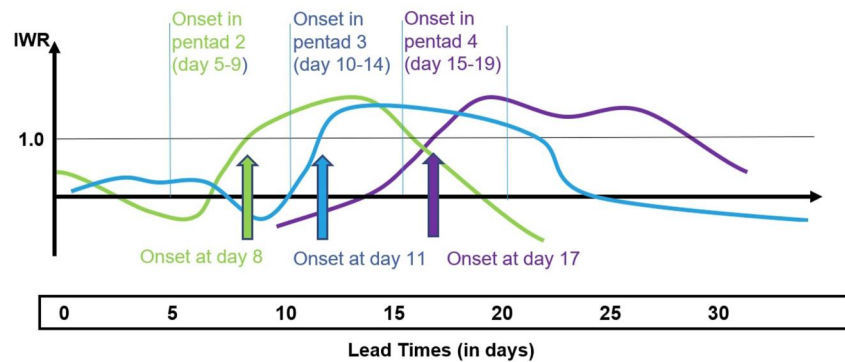


Figure 1. Schematic of weather regime life cycle based on weather regime index I_{wr} . The onset is defined as the day when I_{wr} exceeds a certain threshold. Here, regime onsets in pentad 2 (day 5–9), pentad 3 (day 10–14) and pentad 4 are investigated. They can occur at any day in a given pentad.

2.3. Warm Conveyor Belts

The stages of WCB inflow, ascent, and outflow are identified using a novel framework of convolutional neural networks (CNNs) introduced by Quinting and Grams (2022a). The CNN-based metric (ELIAS2.0) is designed to evaluate WCBs in large data sets at low spatio-temporal resolution for which the original trajectory-based WCB definition (Wernli & Davies, 1997) is not applicable. The method now facilitates for the first time a systematic study of WCBs in a large data set. ELIAS2.0 takes five meteorological parameters as predictors, which are characteristic of each WCB stage. It then predicts conditional probabilities of occurrence of the respective WCB stage from which we derive two-dimensional binary WCB footprints by applying grid point specific decision thresholds. Four of the predictors are derived from temperature, geopotential height, specific humidity and the horizontal wind components at the different isobaric surfaces. For WCB ascent the fifth predictor is the climatological occurrence frequency according to the trajectory-based WCB data. For WCB inflow (outflow) the fifth predictor is the conditional probability of WCB ascent predicted by ELIAS2.0 24 hr before (after) the considered inflow (outflow) time.

The CNN method successfully reproduces the climatological distribution of WCBs (Quinting & Grams, 2022a) which was first found with the trajectory-based approach (Madonna et al., 2014). Moreover, the CNN method skillfully identifies WCBs at instantaneous time steps (Quinting & Grams, 2022a).

2.4. Significance Testing

To corroborate our main findings, we test the ERA-Interim-based anomalies of WCB inflow, WCB outflow, and Z500 for statistical significance using a Monte Carlo approach. Considering all EuBL dates (see Section 2.5.1), we randomly generate 1,000 series of equal sample size. The dates in each random series are composed of a randomly chosen year from the 1997–2017 reforecast period and a randomly chosen day. In order to account for the seasonal variability, each day is chosen from a 14-day period around the corresponding date in the EuBL date series. We then take the average for each of the 1,000 series and determine the 5th and 95th percentiles of the distribution. Anomalies of the original EuBL date series that either fall below the 5th percentile or exceed the 95th percentile are considered to be significant.

2.5. EuBL in Reanalysis and Reforecasts

2.5.1. Forecast Perspective and Lead Times

In our study, we focus on EuBL events in the extended winter period from 1997 to 2017. Following Grams et al. (2017) and Büeler et al. (2021), an EuBL onset is identified at the first time when the respective weather regime index I_{wr} exceeds a threshold of 0.9 and remains above this threshold for at least five consecutive days. In total, there are 38 EuBL “unique events” in ERA-Interim in NDJFM during 1997–2017. In the following, we refer to onset in a given pentad, if the onset date lies within that pentad (see schematic in Figure 1). In order to directly compare ERA-Interim to the reforecasts, we treat ERA-Interim as a “perfect ensemble member” for each forecast initialization time and identify EuBL onset and life cycles in the same manner as for individual ensemble

Table 1

Left: Number of “Unique Events” of Observed EuBL Onsets in ERA-Interim in NDJFM (1997–2017) for Which There Is at Least One Reforecast Initialization Time in the Hits or Misses Category

Hits	Unique events	Forecast perspective	Ensemble members
Pentad 2	34	72	271
Pentad 3	29	45	65
Pentad 4	26	34	41
Misses	Unique events	Forecast perspective	Ensemble members
Pentad 2	38	97	807
Pentad 3	38	98	1,013
Pentad 4	38	98	1,037
False Alarms		Forecast perspective	Ensemble members
Pentad 2		362	728
Pentad 3		540	808
Pentad 4		644	848

Note. There are in total 38 unique EuBL onsets. Middle: Number of initialization times for which at least one ensemble member captures (Hits) [does not capture (Misses)] the EuBL onset according to the “forecast perspective” and number of individual “ensemble members” which capture (Hits) [do not capture (Misses)] the EuBL onset. Bottom: number of initialization times for which at least one member falsely predicts an EuBL onset (“Forecast perspective”) and total number of “ensemble members” falsely predicting an EuBL onset. See Section 2.4 for more explanation.

members of the reforecasts. Thus, we match ERA-Interim to each available reforecast initialization time and lead time. When using ERA-Interim as perfect ensemble member for all available forecasts, the number of EuBL onsets increases because the 38 unique events can be captured multiple times in consecutive forecasts. We call this the “forecast perspective.” In the forecast perspective 98 EuBL onsets are found as the 38 ERA-Interim events are captured on average by 2.6 forecasts (cf. discussion of Table 1 in Section 2.5.2). This approach weights the ERA-Interim events according to the available initialization times of the reforecasts and allows for a direct comparison to the events in the reforecasts. Reforecasts are evaluated in pentad 2 (forecast day 5–9), pentad 3 (day 10–14) and pentad 4 (day 15–19), but the main focus of the study is on pentad 3.

2.5.2. Different Approaches to Link WCBs and EuBL

To assess the role of WCBs for the onset of EuBL, we analyze Z500 and the WCB activity using two different approaches: First, we calculate 5-day mean composites around ERA-Interim onsets to understand characteristics of EuBL in reanalyses and to evaluate the representation of the patterns in the reforecasts at lead times of pentad 2, pentad 3, and pentad 4. We focus on pentads for fixed lead times rather than centered composites around the actual onset date to avoid biases due to mixing different forecast lead times. Second, we investigate the 6 days prior to onset using lagged composites which are stratified according to the individual onset dates in reanalysis and reforecasts. This approach allows for a direct comparison of the time-lagged evolution of the fields while giving hints to potential precursors of the blocked regime.

Furthermore, we distinguish between the ensemble mean of the reforecasts and individual ensemble members which are selected depending on their forecast skill. On the one hand, the ensemble mean of the reforecasts is used to evaluate their ability in representing ERA-Interim EuBL onsets across different lead times. On the other hand, single ensemble members from different initialization times are grouped together, depending on their ability to represent EuBL to explore potential deficiencies in the model related to the link of WCB activity and blocking onset. Ensemble members that correctly (within 2 days of the verifying date) capture an ERA-Interim EuBL onset are defined as “Hits,” members which do not capture the onset as “Misses.” Furthermore, we include all ensemble members in our study that predict an EuBL onset while no event is analyzed in ERA-Interim (“False Alarms”).

As stated above, we find 38 “unique EuBL events” in ERA-Interim in the 20-year period 1997–2017 which can occur in either pentads 2, 3, or 4 of the available reforecasts when ERA-Interim is used as perfect ensemble member. Accounting for consecutive forecast initialization times according to the “forecast perspective,” these are captured in 98 of the available reforecasts irrespective of the pentad (not shown). Thus, 98×11 ensemble members = 1,078 individual forecasts could either identify (Hit) or not identify (Miss) these EuBL onsets (cf. Table 1 last column sum of Hit and Misses for different pentads, and discussion below). In addition, forecasts can issue a false alarm.

For 34 out of the 38 unique ERA-Interim events, there is at least one ensemble member in at least one of the available initialization times that correctly captures the EuBL onset (Hit) at a leadtime of pentad 2 (4 unique events are completely missed) (Table 1 top row). This number of captured unique events decreases for onsets at lead times of pentad 3 and 4 (29 and 26 unique events, respectively). In fact, each unique EuBL event is captured by more than one forecast since the reforecasts are initialized multiple times per week (see “forecast perspective”) with 72/45/34 initial times with a Hit for EuBL onsets at lead times of pentad 2/3/4. When the EuBL is captured by these forecasts, most of the times 1–2 ensemble members correctly predict the onset in pentad 2. However, there are even events that are correctly predicted by 3–11 ensemble members, which results in a total of 271 individual ensemble members (25% of all possible ensemble members) capturing an EuBL onset in pentad 2. For correctly predicted onsets in pentad 3, this number decreases to 65 (6%) with the events being mostly captured by 1–2 ensemble members and some by 3–4. In pentad 4, there are 41 ensemble members (3% of all possible ensemble members) that capture the 26 unique EuBL events. These numbers illustrate that the accurate

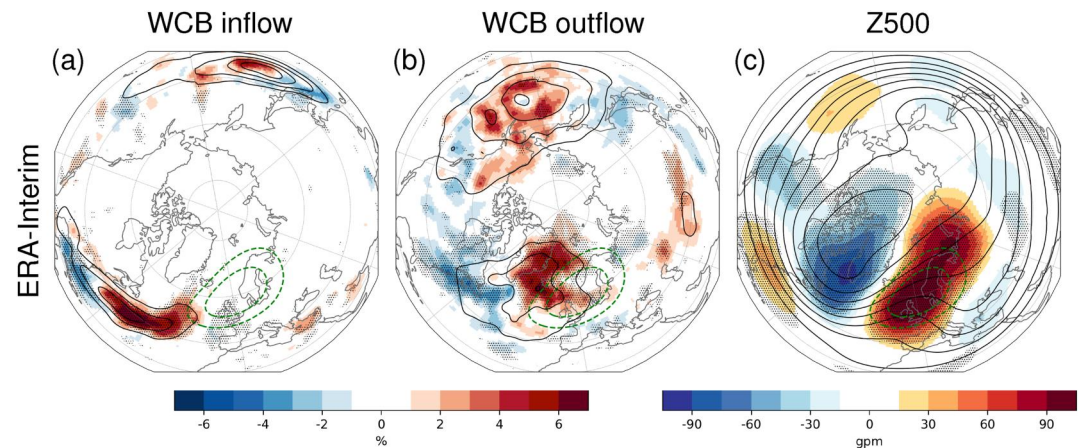


Figure 2. WCB inflow (a), WCB outflow (b), and 500 hPa geopotential height anomalies (c) anomalies (shading) around EuBL onsets in ERA-Interim (5-day mean in pentad 3; NDJFM, 1997–2017; ERA-Interim treated as the “perfect ensemble member”). Black contours indicate absolute fields (frequencies ranging from 5% to 20% every 5% in (a) and (b), and 5100 to 5800 gpm, every 100 gpm in (c)). Black dots show statistical significance of positive/negative anomalies determined through a Monte Carlo test at the 95% and 5% confidence levels. Green contours indicate geopotential height anomalies (50,100 gpm) for all ERA-Interim EuBL cases from 1979 to 2015.

representation of EuBL becomes more challenging with forecast lead time. Still, in pentad 4, 26 out of the 38 unique events are captured by at least one ensemble member, which provides robustness to our further analysis.

The Misses category contains all ensemble members which do not predict the onset of the observed EuBL event (middle rows in Table 1). For all pentads, all of the 38 observed unique events belong to Misses category, meaning that there is at least one ensemble member in at least one available forecast initialization time missing the onset. In fact, except for pentad 2, in all of the 98 available reforecasts there is at least one member missing the onset (forecast perspective). For pentad 2, there is one initial time with all 11 members correctly capturing the onset, therefore only 97 of the available 98 initialization times belong to the Misses category. We also note that the number of “ensemble members” in Hits and Misses must add up to 1,078 which is the number of available individual ensemble members (see begin of this section). There is a very high number of individual ensemble members missing EuBL onset, consistent with the fact that on average only 1–2 ensemble members belong to the Hits category. Naturally, the number of ensemble members in the Misses category is highest for onsets in pentad 4 when the number of Hits is lowest.

Lastly, the ensemble members which predict an EuBL onset that is not observed in ERA-Interim make up the False Alarms category (bottom rows in Table 1). Out of the 1,641 forecast initialization times in the reforecast period, there are 362 with at least one ensemble member with a False Alarm in pentad 2 (forecast perspective). The number of forecast initialization times with False Alarms is even higher in pentads 3 and 4. In fact on average 1–2 ensemble members in each of these forecasts issue a false alarm although we found individual initial times with 3–8 false alarm members in pentad 2.

3. The Role of WCBs for EuBL Prediction

In this Section, we start our exploration of the potential link between WCB activity and EuBL onset by first focusing on ERA-Interim and the ensemble mean reforecast. To this end we investigate the spatial patterns of Z500, as well as WCB inflow and outflow occurrence frequency anomalies around EuBL onsets in pentad 3 (10–14 days) for both data sets.

The 5-day mean ERA-Interim Z500 field shows a significant positive Z500 anomaly of more than 90 gpm extending from western Europe to Scandinavia (Figure 2c) following the time of EuBL onset. This anomaly reflects the developing block over Europe. Upstream, a negative anomaly (–60 to –90 gpm) indicates a trough over the western and central North Atlantic. The strong Z500 anomalies are in line with the climatological pattern of the EuBL regime (green dashed contour in Figure 2, see Grams et al. (2017)). The large-scale circulation over North America and the North Pacific indicates a weakly undulated jet stream (dense isohypses, black in Figure 2c)

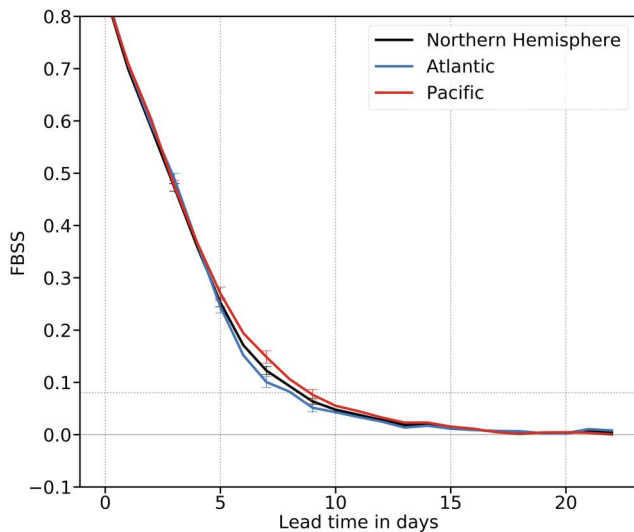


Figure 3. Area-averaged Fair Brier Skill Score (*FBSS*) for DJF 1997–2017 at different forecast lead times for WCB outflow. The area-average of the *FBSS* is computed over the North Atlantic (20–90N, 100W–20E), North Pacific (20–90N, 120E–120W) and for the entire Northern Hemisphere. Error bars centered on forecast lead times day 3, 5, 7, and 9 show the difference between the 10 and 90th percentile of the sampled data (variability of the *FBSS*) and are used to estimate the significant differences between the ocean basins.

with an anomalous Rossby wave packet along the midlatitude jet (reflected in pairs of negative Z500 anomalies over the western part of the North Pacific/western North America and positive Z500 anomalies over the eastern North Pacific/East coast of North America). Anomalies over North America and the North Atlantic are statistically significant. We note that Rossby wave activity upstream of blocking over Europe and the embedment of blocking into an amplified Rossby wave train emerging from the Caribbean has already been established by various studies (e.g., Altenhoff et al., 2008; Michel & Rivière, 2011). We further discuss upstream precursors and the role of Rossby wave activity in Section 5.

Significantly enhanced WCB inflow occurs during the EuBL onset in a region stretching from south of Newfoundland into the central North Atlantic (5-day mean anomalies of 4%–8%; Figure 2a). The strongest WCB inflow anomalies are located just south and ahead of the amplified North Atlantic trough (negative Z500 anomaly in Figure 2c). The air masses typically converge in the WCB inflow region and are subsequently lifted to the mid and upper troposphere due to strong vertical lifting in the vicinity of surface cyclones. The air masses then reach the upper troposphere further to the northeast of the inflow region. Indeed, around EuBL onsets, significantly enhanced WCB outflow frequencies occur northeast of the inflow region in an area around eastern Greenland, Iceland and over the Norwegian Sea (Figure 2b). Here, the 5-day mean outflow frequency anomalies reach 4%–6%, that is, more than double the climatological frequency in that region. The air masses likely influence the upper-level ridge building (cf. Grams et al., 2018; Steinfeld & Pfahl, 2019, and summary in introduction for the physical processes involved), which subsequently leads to the onset and persistence of the block over Europe.

In summary, we find a co-occurrence of WCB outflow and the emergence of a strong positive Z500 anomaly in the region of the block in the climatological composite of all EuBL onsets in NDJFM 1997–2017. Although we can not infer causality from these results, they suggest that WCBs might play a vital role in the formation of the blocked regime over Europe consistent with prior work (Pfahl et al., 2015; Steinfeld & Pfahl, 2019).

Before investigating how well these patterns are represented in IFS reforecasts, we evaluate the overall forecast skill for predicting WCBs (Figure 3). We here discuss the Fair Brier Skill Score (*FBSS*) (Ferro, 2014) for WCB outflow frequencies based on the CNN-based WCB metric ELIAS2.0 (Quinting & Grams, 2022a). This also provides an update for the WCB skill assessment with an earlier version of the Eulerian WCB metric using logistic regression instead of the CNN (Wandel et al., 2021). This analysis shows that the WCB forecast skill vanishes at medium-range forecast lead times in forecast week 2 (between day 8–14) with the exponential decay of WCB skill leveling off between pentad 2 (day 5–9) and 3 (day 10–14). While pentad 2 still shows some WCB skill, forecasts for pentad 3 are only slightly better than a climatological reference forecast. Therefore, to be able to distinguish between pentad 2 with some skill and pentad 3 with hardly skill, we focus here on pentads rather than weeks.

In the following, we briefly evaluate how well the ensemble mean reforecasts can predict the large-scale circulation (in terms of Z500) anomalies and WCB activity around EuBL onsets as found for ERA-Interim (Figure 2). We show the same fields as in Figure 2 but for the ensemble mean of reforecasts and EuBL onsets during pentads 2, 3, and 4 (Figure 4). In pentad 2 the ensemble mean reforecast is able to represent WCB inflow, its associated outflow and the downstream Z500 pattern of the incipient block accurately (Figures 4a–4c). Overall the anomalies are somewhat weaker compared to ERA-Interim (Figure 2). This has to be expected as we look at the ensemble mean with only 25% of the ensemble members correctly predicting EuBL onset in pentad 2 (cf. discussion of Table 1 in Section 2.5.2). In pentad 3, and in particular in pentad 4 the anomaly patterns are hardly discernible from climatology, reflecting the little skill of the ensemble mean to predict EuBL onset.

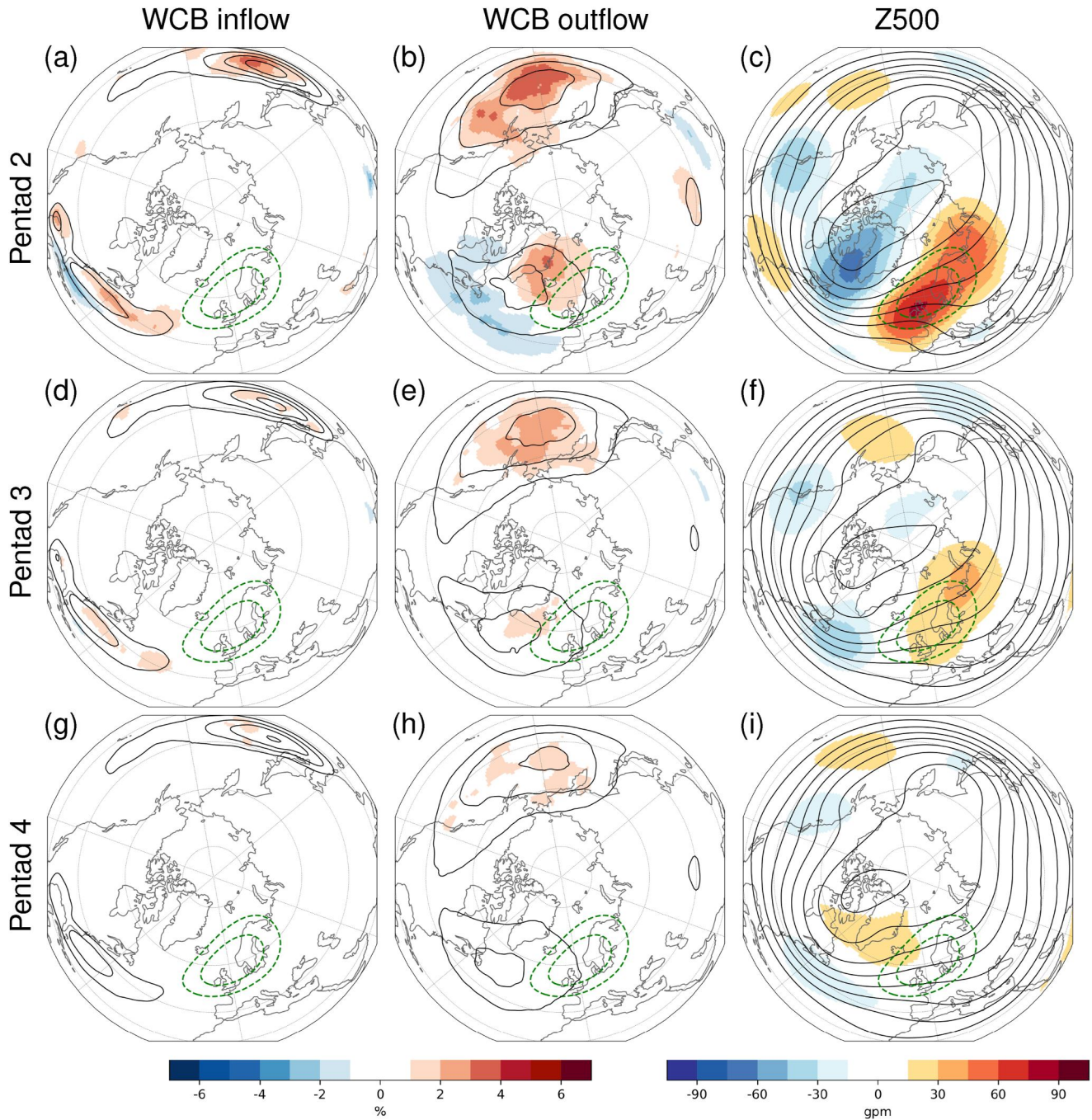


Figure 4. Ensemble mean prediction (ECMWF's IFS reforecasts; NDJFM 1997–2017) of EuBL onsets in ERA-Interim in (a–c) pentad 2, (d–f) pentad 3, and (g–i) pentad 4. Plots show 5-day mean anomalies (shading) of ensemble mean forecasts in different pentads for (a, d, g) WCB inflow, (b, e, h) WCB outflow and (c, f, i) Z500, as well as 5-day mean WCB frequencies (black contours; 5%, 10%, 15%, 20% in (a, b, d, e, g, h) and Z500 fields (black contours; 5100–5800 gpm, every 100 gpm in (c, f, i). Green contours as in Figure 2.

In summary, we find that the IFS ensemble mean reforecast fails predicting the Z500 anomaly associated with EuBL onset from pentad 3 onwards along with a lack of predicting the co-occurring WCB activity. Still in pentad 2, we find a consistent pattern of WCB inflow and outflow upstream of the emerging Z500 anomaly with a somewhat different spatial structure of WCB outflow frequency anomalies in reforecasts compared to ERA-

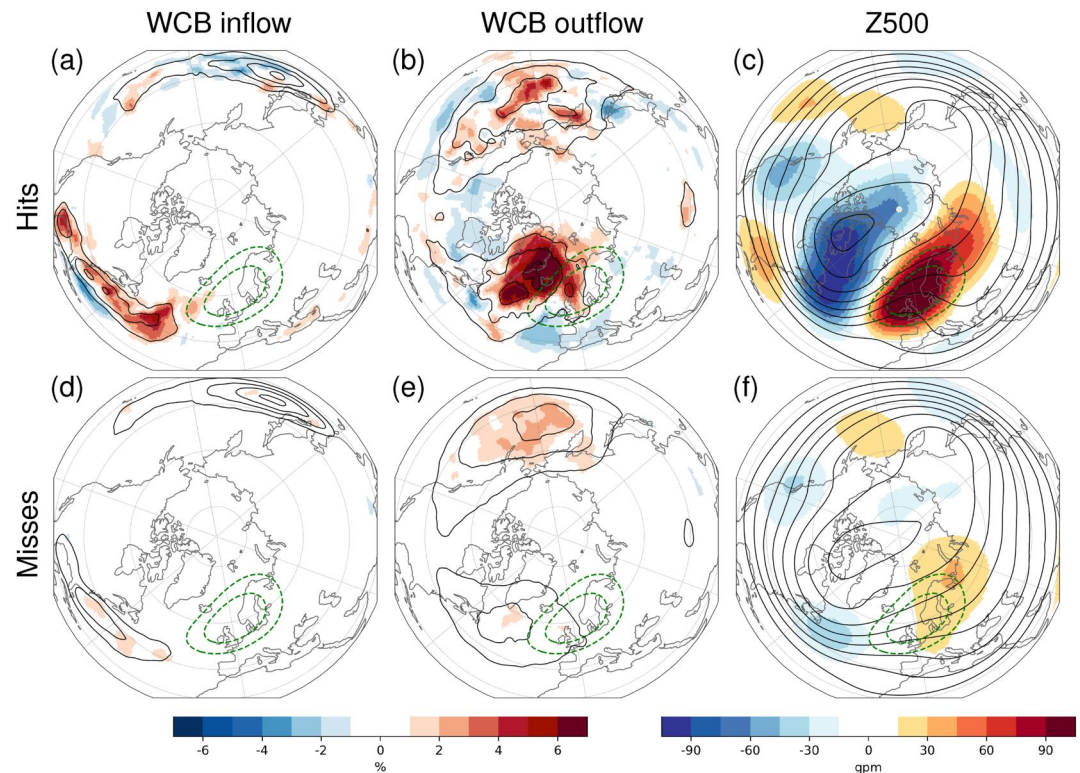


Figure 5. (a–c) Ensemble members with a correct representation of ERA-Interim EuBL onset (Hits, 65 members) and (d–f) ensemble members missing ERA-interim onsets (Misses, 1,013 members) in pentad 3 (5-day mean of (a, d) WCB inflow, (b, e) WCB outflow and (c, f) Z500 anomalies (shading) and absolute frequencies (contours) as in Figure 4 (ECMWF’s IFS reforecasts, NDJFM, 1997–2017)). Green contours as in Figure 2.

Interim. Interestingly, the reforecast consistently shows an upstream Rossby wave pattern over North America also in pentad 3.

4. The Importance of Accurate WCB Prediction

4.1. The Link Between WCB Activity and Correct Predictions of EuBL Onset

The previous section established that WCB outflow is enhanced upstream of the positive Z500 anomaly associated with EuBL in both ERA-Interim and IFS reforecasts at least for pentad 2. Comparing ensemble members which accurately predict (Hits) EuBL onset, do not predict it (Misses), or predict EuBL onset when no onset is observed (False Alarms) allows us to shed more light on the question if the WCB activity is mere coincidence or more systematically linked to EuBL onset. Thus, we divide the individual ensemble members in the three categories depending on their ability to predict EuBL onset (see Section 2.5.2).

We now focus on pentad 3 in which 65 ensemble members capture the observed EuBL onset. The analysis of the Z500 field shows large positive Z500 anomalies of more than 90 gpm centered over the British Isles (Figure 5c) consistent with the circulation anomalies around the onset in ERA-Interim (Figure 2c). The negative anomalies over the western and central North Atlantic are even larger for the Hits compared to ERA-Interim. In line with the Z500 pattern over the North Atlantic and Europe, we find strongly enhanced WCB frequencies over the central North Atlantic for the WCB inflow and centered around Greenland and Iceland for the WCB outflow (Figures 5a and 5b). As for Z500, the WCB anomaly patterns strongly resemble the 5-day mean frequency anomalies around EuBL onsets in ERA-Interim (Figures 2a and 2b). This finding holds even for the 41 ensemble members with a hit in pentad 4 (Figures S1a–S1c in Supporting Information S1).

However, the bulk of ensemble members (1,013 of 1,078) misses the EuBL onset in pentad 3 and consistently these ensemble members only show a weak positive Z500 anomaly which is displaced to the northeast compared

to ERA-Interim (Figure 5f). Interestingly, there is hardly any enhanced WCB activity in the North Atlantic region (Figures 5d and 5e). Likewise in pentad 4, ensemble members in the Misses category fail predicting the Z500 pattern and do not capture the enhanced WCB activity over the North Atlantic at all (Figures S1d and S1e in Supporting Information S1).

Our findings are in line with the climatological evidence regarding the chain of physical processes by which LHR can affect blocking (e.g., Grams & Archambault, 2016; Hauser et al., 2023b; Pfahl et al., 2015; Steinfeld & Pfahl, 2019; Teubler et al., 2023). We conclude that there is a strong link between the correct representation of local WCB activity in the North Atlantic-European region and the correct representation of the large-scale circulation around EuBL onsets in NWP models. This holds even for lead times beyond 10 days when the average WCB forecast skill has already vanished and the prediction of EuBL becomes increasingly challenging (Figure S1 in Supporting Information S1). Thus, a correct prediction of WCBs could provide a window of forecast opportunity for the prediction of blocked regimes over Europe even on sub-seasonal time scales.

4.2. Time-Lagged Evolution Prior to EuBL Onset

So far, we analyzed the onset of EuBL based on ERA-Interim, the ensemble mean of the reforecast and for different subcategories. While this approach gives an overview over the fields around the onset, it does not solve the chicken-and-egg problem: WCB activity might emerge prior to the onset of the regime and, via the chain of processes described in the introduction, directly result in ridge building and the development of the block over Europe. Or the block could deviate cyclones over the North Atlantic in a way so that enhanced WCB activity occurs upstream of the block. In order to shed light on this problem, we calculate lagged composites of WCB frequency anomalies in ERA-Interim and for the three subcategories of the reforecasts (False Alarms, Hits, and Misses) prior to EuBL onset. Again we focus on results for EuBL onsets in pentad 3.

The WCB outflow activity in ERA-Interim prior to EuBL onsets is significantly enhanced over eastern Canada 6 to 4 days before the onset (Figure 6a). On the other hand, frequencies are below average over the central North Atlantic around Iceland and Greenland. Subsequently, the enhanced outflow activity over eastern Canada shifts eastwards 4 to 2 days prior to the EuBL onset (Figure 6e). Here, WCB frequencies are significantly enhanced from eastern Canada and the southern tip of Greenland to western Europe (anomalies around 5%). 2 to 0 days before the EuBL onset, we find a northeastward shift of the main WCB activity with highest and significantly positive frequency anomalies over the Norwegian Sea and the northwestern part of Europe (Figure 6i). Outflow frequencies are significantly lower than normal over the western North Atlantic.

In summary, in ERA-Interim, we find significantly enhanced WCB outflow frequencies already during the six days before the onset of EuBL and well before a positive Z500 anomaly is evident in the European region. This enhanced WCB outflow gradually leads to ridge building upstream of the EuBL region. The associated upper-tropospheric anticyclonic circulation anomaly propagates downstream (Figure S4 in Supporting Information S1) and establishes a positive Z500 anomaly in the region of the incipient block over Europe around onset (Figure S4i in Supporting Information S1). Thus, it is the WCB activity and associated outflow that precedes the onset of blocking. Interestingly, also over the North Pacific WCB activity is enhanced in the 6 days prior to EuBL onset, pointing toward a potential downstream development, which we discuss in more detail in Section 5.

We now investigate to what extent the different subcategories of the reforecasts capture the enhanced WCB frequencies over the North Atlantic and Europe prior to EuBL onsets. In the False Alarms category only 4 to 2 days (Figure 6f), and in particular in the 2 days (Figure 6j) prior to a wrongly predicted EuBL onset, enhanced WCB activity emerges over Southern Greenland. The outflow anomaly is shifted westward and the branch toward Northwestern Europe is missing compared to ERA-Interim (cf. Figures 6i and 6j). Thus, in the case of False Alarms the model predicts a non-observed EuBL onset via a different pathway. Interestingly, also the upstream WCB activity over the North Pacific is weaker for False Alarms compared to ERA-interim.

Ensemble members not predicting EuBL onset when they should (Misses category, Figures 6d, 6h, and 6l) only capture the initially enhanced WCB activity over eastern North America 6 to 4 days before onset, but later no anomalous WCB activity occurs, despite some signals upstream over the North Pacific.

In contrast to False Alarms and Misses, the Hits category reflects the anomalous WCB activity compared to ERA-Interim remarkably well (Figures 6c, 6g and 6h). Not only do ensemble members in the Hits category reflect the anomalous WCB activity upstream over the North Pacific, but also the local flow amplification in the North

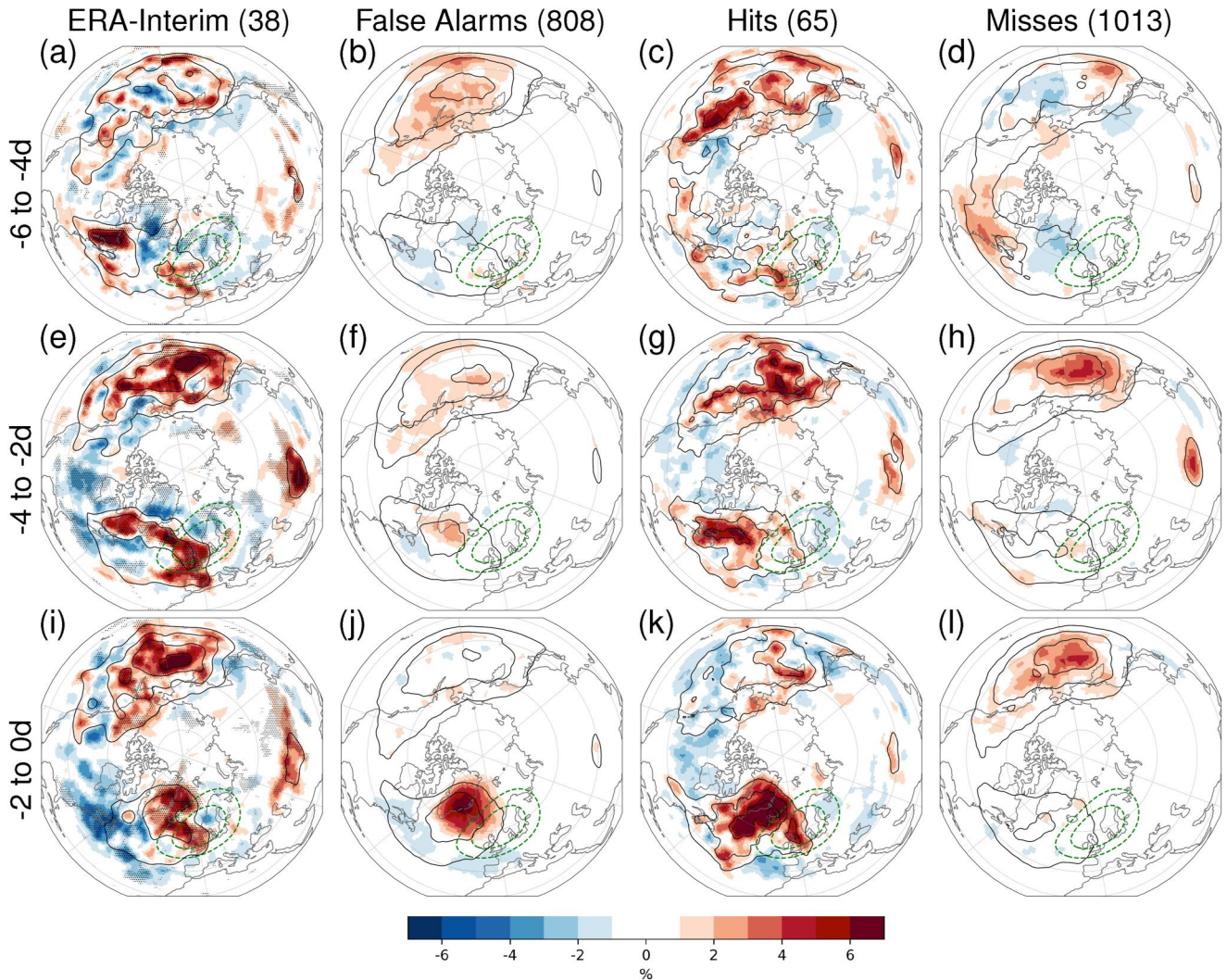


Figure 6. WCB outflow frequency anomalies (shading) 6 to 4 days (a–d), 4 to 2 days (e–h), and 2 to 0 days (i–l) prior to EuBL onset in pentad 3 in (a, e, i) ERA-Interim (NDJFM; 1997–2017), (b, f, j) False Alarms, (c, g, k) Hits, (d, h, l) Misses (ECMWF’s IFS reforecasts; NDJFM, 1997–2017). Numbers on top indicate number of members in the respective category (see Table 1). Black dots in (a, e, i) indicate statistical significance of positive/negative anomalies determined through a Monte Carlo test at the 95% and 5% confidence levels. Black contours indicate absolute WCB outflow (5%, 10%, 15%, 20%), green contours as in Figure 2.

Atlantic region is captured: 6 to 4 days prior to EuBL onset the anomalous WCB activity emerges over Newfoundland and the North Atlantic albeit somewhat weaker than in ERA-Interim (Figure 6c). 4 to 2 days prior to onset the WCB activity expands towards southern Greenland (Figure 6g). In the 2 days prior to EuBL onset the model even captures the two regions of strongly enhanced WCB outflow over the Norwegian Sea and in a branch toward Northwestern Europe (Figure 6k).

We note that the results in Figure 6 are qualitatively very similar for ERA-Interim, as well as the Hits and False Alarms categories when using onsets in pentad 2 or 4 (Supplement Figures S2 and S3 in Supporting Information S1). However, WCB frequencies are slightly higher for the Misses category for onsets in pentad 2 (Figures S2d, S2h, and S2l in Supporting Information S1) and even lower for onsets in pentad 4 (Figures S3d, S3h, and S3l in Supporting Information S1). This is in line with the WCB forecast skill, which shows that accurate predictions are still possible in pentad 2 (Figure 3).

All in all, the lagged analysis of WCB activity before EuBL onsets shows that there is a distinct pattern of anomalous WCB activity emerging from the eastern Coast of North America in the 6 days prior to EuBL onset. Remarkably this pattern is only reflected in reforecasts correctly predicting EuBL onset. The Misses category

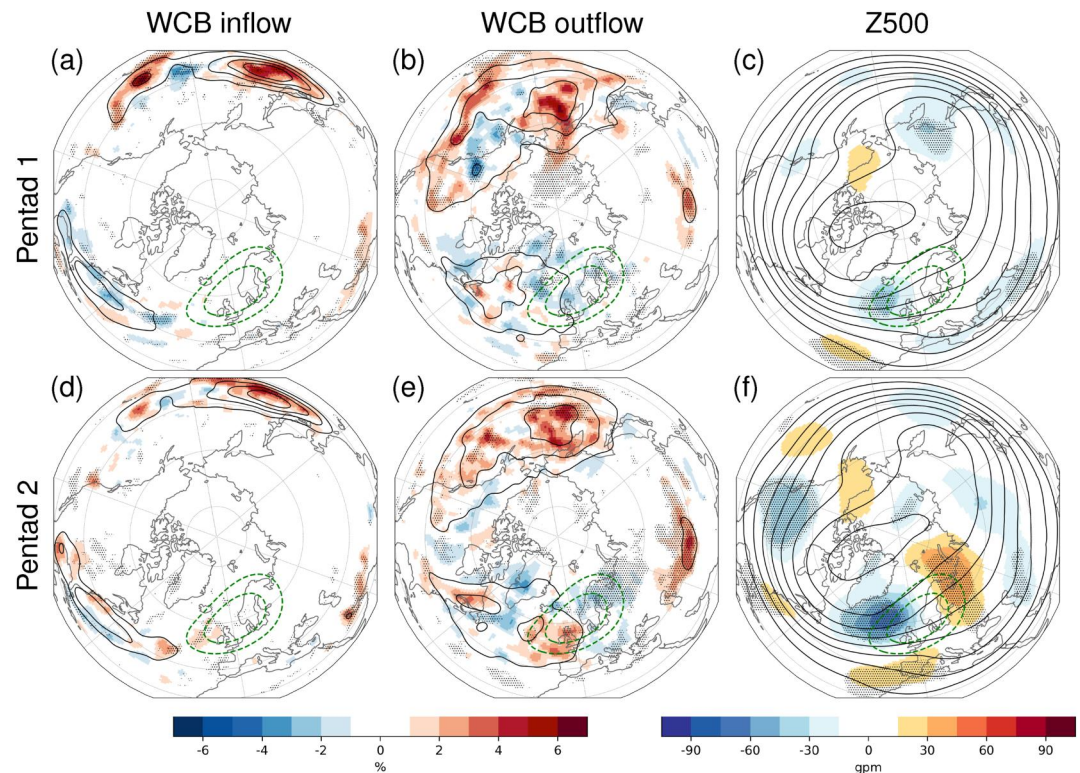


Figure 7. Evolution of 5-day mean (a,d) WCB inflow, (b, e) WCB outflow and (c, f) Z500 in ERA-Interim in (a–c) pentad 1 and (d–f) pentad 2 before ERA-Interim EuBL onsets in pentad 3 (ERA-Interim treated as the “perfect ensemble member”). WCB and Z500 anomalies (shading), absolute fields (contours), black dots and green contours as in Figure 2.

does not feature anomalous WCB activity. Erroneously predicted EuBL onsets in the False Alarm category establish blocking via a different pathway with outflow focused more westward over Greenland.

The fact that WCB activity is already enhanced up to 6 days prior to the onset of EuBL corroborates its likely important contribution to the establishment of a persistent blocked regime over Europe. In addition, we show that only if forecasts capture this WCB activity, blocking is correctly predicted. Our qualitative result is further confirmed quantitatively in a quasi-Lagrangian potential vorticity framework recently established by Hauser et al. (2023b) and Hauser (2023).

5. The Role of Upstream Precursors

We now focus on the role of upstream precursors from the North Pacific for the prediction of EuBL. So far, we found evidence for concomitant WCB activity over the North Pacific region around EuBL onsets (Figures 2a and 2b), which is linked to Rossby wave activity emerging from the western North Pacific (Figure 2c).

As the downstream propagation of Rossby waves from the North Pacific toward Europe typically requires 5–10 days, we now investigate the evolution of WCB activity and Z500 fields in ERA-Interim in pentads 1 and 2 prior to EuBL onsets in pentad 3. During both pentads positive WCB inflow anomalies are found over the western North Pacific (frequencies around 20%, anomalies around 4%) and over the central North Pacific (anomalies around 4%–6%) (Figures 7a and 7d). In both regions, this might be explained by higher cyclone activity and associated WCBs ahead of upper-level troughs as indicated by weak but non-significant negative Z500 anomalies (Figures 7c and 7f). Consistent with the WCB inflow, enhanced WCB outflow occurs downstream over the northern part of the central Pacific and further south over the eastern part of the ocean basin (Figures 7b and 7e). Over the North Atlantic WCB activity is weak and only partly significantly different from climatology.

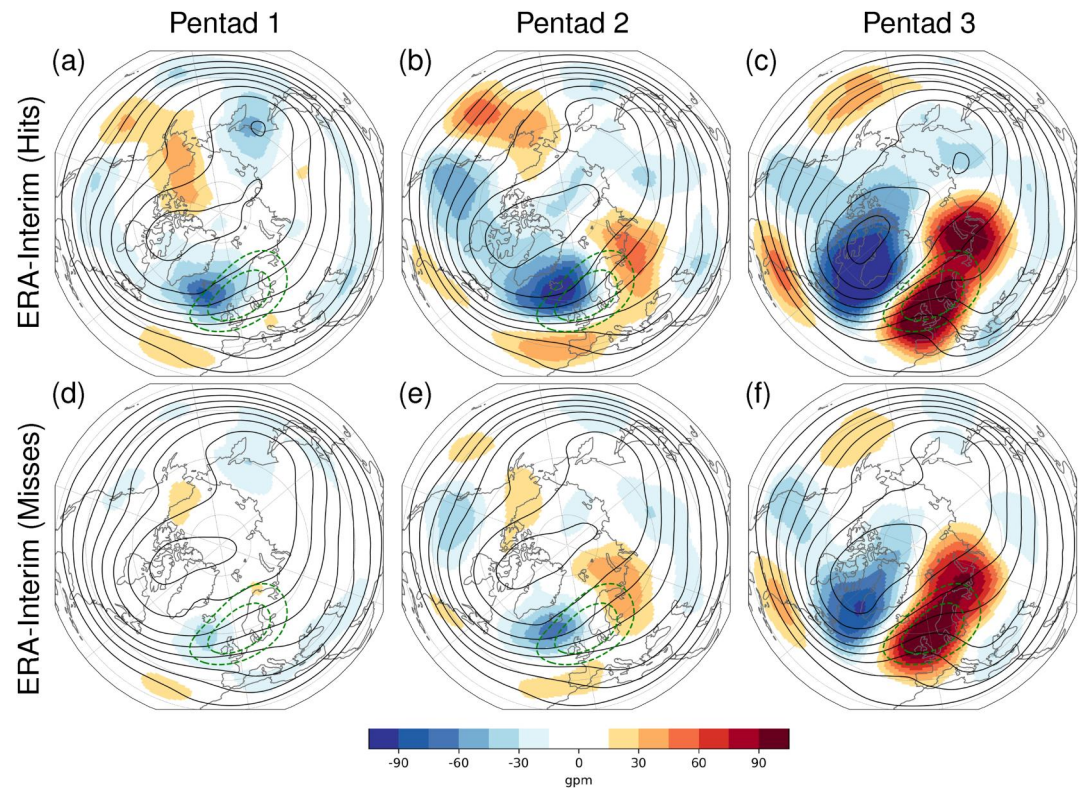


Figure 8. Evolution of 5-day mean Z500 in ERA-Interim weighted with the number of ensemble members in the Hits category (a–c; 29 unique events, 65 ensemble members, see Table 1) and (d–f) Misses (d–f; 38 unique events, 1,013 ensemble members) for each respective forecast initial time in (a, d) pentad 1 and (b, d) pentad 2 before ERA-Interim EuBL onsets in (c, f) pentad 3. Z500 anomalies (shading), absolute fields (contours) and green contours as in Figure 2.

In summary, WCB activity is enhanced over the North Pacific 5–10 days prior to EuBL onset. However, WCB frequency anomalies as well as Z500 anomalies are hardly significant making it difficult to identify a clear precursor pattern.

We now evaluate if precursor patterns differ depending on the ability of IFS reforecasts to correctly predict EuBL onset in pentad 3. Therefore, we first contrast ERA-Interim Z500 fields for two subcategories based on Hits and Misses in reforecasts. Note that we weight unique EuBL events according to the ability of the reforecast in predicting the respective EuBL onset. Here, this ability is measured by the number of ensemble members in the Hits and Misses category for each event. If an EuBL event is well predicted (many members in the Hits category), it weights more in the ERA-Interim Hits subcategory and weights less heavy in the Misses subcategory. On the other hand, if an EuBL event is poorly predicted (only few or no members in the Hits category), it is weighted less heavily in the ERA-Interim Hits subcategory and more heavily in the Misses subcategory. The subcategory based on the Hits contains 29 of the 38 unique EuBL events while the subcategory based on the Misses contains all 38 events.

Around EuBL onset in pentad 3, both subcategories show the developing block over Europe with similar positive Z500 anomalies (Figures 8c and 8f). Both subcategories also show the concomitant amplified Rossby wave pattern over the North Pacific and North America (cf. also Figure 2c). However, upstream Z500 anomalies are slightly stronger when reforecasts successfully predict EuBL (Hits) (Figure 8c). This becomes even more noticeable in pentads 2 and 1 prior to the EuBL onset. If reforecasts miss to predict EuBL onset, the upstream anomalous Rossby wave pattern is almost absent (Misses, Figures 8d and 8e). In contrast, a marked upstream Rossby wave pattern is evident in the subcategory based on Hits (Figures 8a and 8b) which emerges from the western North Pacific already in pentad 1.

Associated with the Rossby wave pattern in the Hits subcategory is anomalously high WCB activity over the North Pacific (Figures S6a and S6b in Supporting Information S1). The collocation of above average Z500 and

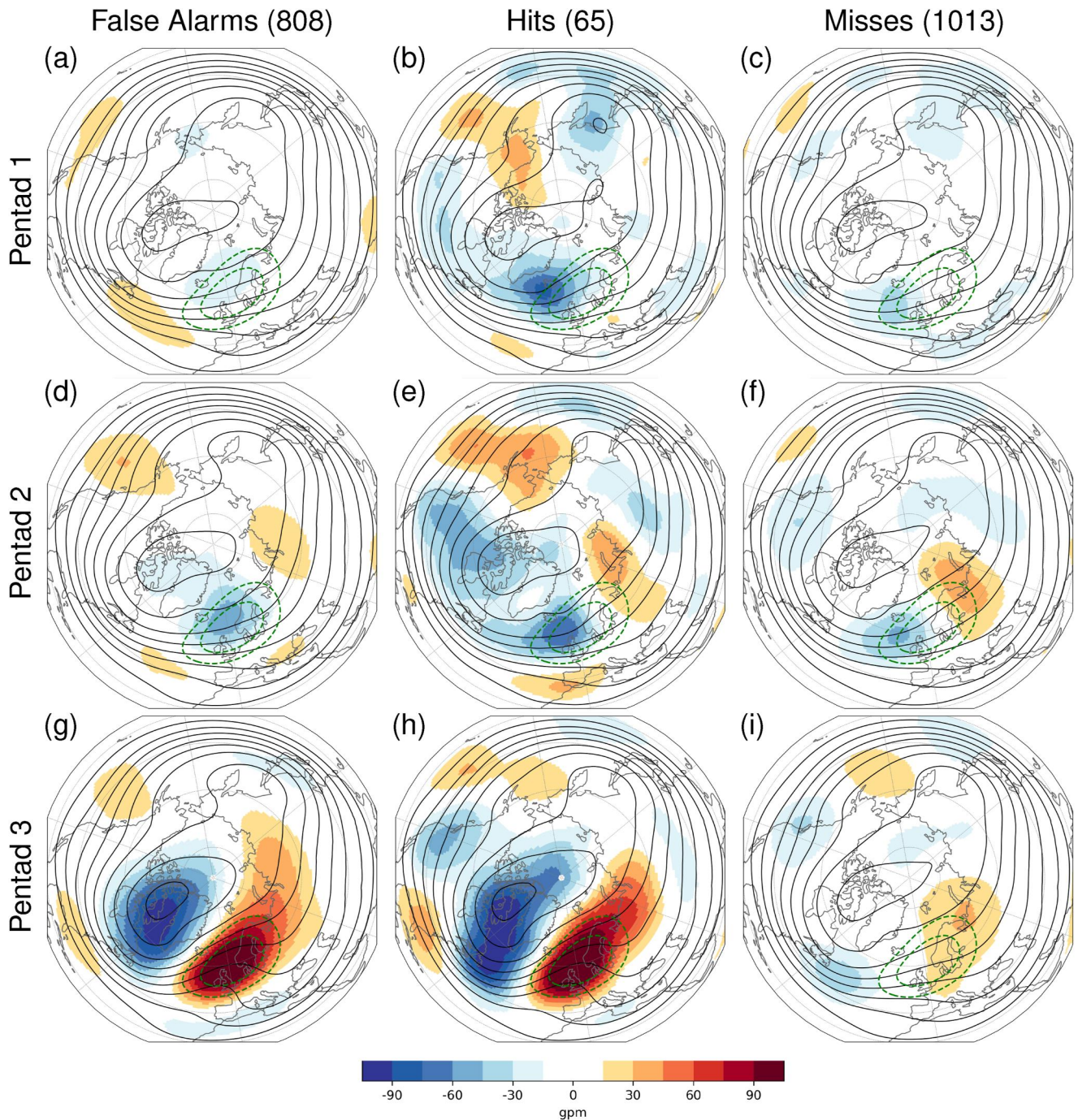


Figure 9. Evolution of 5-day mean Z500 anomalies (shading) for (a, d, g) False Alarms, (b, e, h) Hits, and (c, f, i) Misses (ECMWF's IFS reforecasts, NDJFM, 1997–2017) in (a–c) pentad 1, (d–f) pentad 2, and (g–i) pentad 3 prior to and around EuBL onsets in pentad 3. Numbers on top indicate number of members in the respective category (see Table 1) and black contours show absolute Z500 fields (5100–5800 gpm, every 100 gpm). Green contours as in Figure 2.

anomalously high WCB outflow frequencies over the eastern North Pacific indicate that, following the process chain described in the introduction, diabatic heating associated with WCBs contributes to the strengthening of the positive Z500 anomaly. Likewise, pentad 2 is characterized by a positive WCB outflow frequency anomaly over eastern North America (Figure S6b in Supporting Information S1) which is in line with a slightly enhanced positive Z500 anomaly in the same region. Though positive WCB inflow and outflow anomalies are also found over the North Pacific during pentads 1 and 2 of the Misses category (Figures S5d, S5e and S6d, S6e in

Supporting Information S1), these anomalies are smaller than in the Hits category. Together with a mean Z500 close to climatology this indicates less favorable conditions for WCB development that would further amplify the flow.

These results suggest that EuBL events with a Rossby wave packet emerging from the North Pacific already in pentad 1 enable a successful prediction of EuBL onsets in ECMWF's IFS reforecasts, while the model misses the onset prediction in the absence of this Rossby wave packet. That the presence of long-lived Rossby wave packet emerging from the North Pacific are associated with enhanced predictive skill over the North Atlantic-European region is in line with Grazzini and Vitart (2015). It overall indicates an enhanced intrinsic predictability in such situations which may be favored by modes of intraseasonal variability such as the Madden-Julian Oscillation (MJO) that importantly modulates the North Pacific WCB activity (Quinting et al., 2024). With regard to the practical predictability and the case that small-scale processes in WCBs are only insufficiently reproduced in NWP models, the increased WCB activity on the other hand may reduce this increased intrinsic predictability.

Lastly, we directly evaluate the large-scale circulation in IFS reforecasts for the three subcategories Hits, Misses, and False Alarms, in pentads 1 and 2 prior to EuBL onsets in pentad 3. Recall that False Alarms show EuBL onset independent of ERA-Interim. Consistently, the Z500 anomalies for False Alarms show the trough-ridge couplet typical for EuBL onset in pentad 3 (Figure 9g). However, upstream anomalies are weak and there is no distinct upstream Rossby wave pattern in pentads 1 and 2 (Figures 9a and 9d). IFS reforecasts missing EuBL onset in pentad 3 strongly underestimate the developing block over Europe (Figure 9i) and also feature only weak and indistinct upstream anomalies (Figures 9c and 9f). However, successful reforecasts (Hits) not only correctly represent the Z500 anomalies at EuBL onset in pentad 3 (Figure 9h), they also show a marked concomitant upstream Rossby wave pattern, evident in pentad 2, too, and emerging from the western North Pacific in pentad 1 (Figures 9b and 9e). It is noteworthy, that the composites of successful EuBL onset predictions (Hits, Figures 9b, 9e and 9h) hardly differ from the corresponding Z500 patterns in ERA-Interim (Figures 8a–8c). These results corroborate that an upstream Rossby wave packet emerging from the western North Pacific 5–10 days prior to EuBL onset provides an additional potential window of forecast opportunity for EuBL in pentad 3.

6. Conclusions

In this study, we investigate Z500 and WCB activity around the onset of blocked weather regimes over Europe (EuBL) in ECMWF's IFS sub-seasonal reforecasts and ERA-Interim reanalyses (NDJFM; 1997–2017). EuBL onset is not well predicted by the reforecasts at 10–14 days lead time, which is partly due to its low intrinsic predictability (Faranda et al., 2016; Hochman et al., 2021). Our study newly suggests that for lead times beyond 10 days the model struggles predicting the flow amplification, in particular the ridge building prior to EuBL onset. We find that this is due to a strong link between the Rossby wave amplification around EuBL and enhanced WCB outflow over the central and eastern North Atlantic well before the block establishes. The model misrepresents WCB activity, which ultimately dilutes skill for EuBL forecasts. This mechanistic link between upstream WCB activity and blocking over Europe, which we found and described here in a qualitative way based on composites has recently been confirmed by Hauser et al. (2023b) and Hauser (2023) in a quantitative potential vorticity framework.

The role of WCB activity for EuBL onset was evident independent of different perspectives taken: For EuBL onsets at early lead times in pentad 2 (5–9 days), the ensemble mean of the reforecasts can predict the WCB activity and incipient block relatively well. This is in line with the overall WCB forecast skill, which is still sufficient on these time scales (Wandel et al., 2021). However, onsets in pentad 3 (10–14 days) and pentad 4 (15–19 days) are challenging for the NWP model. Consistently, the model strongly underestimates WCB activity and subsequently the developing block prior to onsets in pentad 3 and on average misses onsets in pentad 4 completely.

In addition stratification of the reforecasts according to Hits, Misses, and False Alarms of EuBL onset in pentad 3 and pentad 4 shows different pathways toward EuBL onset. For successful predictions of EuBL onset (Hits), the model accurately represents the enhanced WCB activity prior to EuBL onset, whereas for Misses it completely misses WCB activity. Finally, time-lagged analysis reveals that the enhanced WCB activity emerges from the western North Atlantic already 6 days prior to EuBL onset - well before any indication of blocking over Europe. Thus, a correct representation of WCB activity provides a potential window of forecast opportunity for EuBL forecasts beyond 10 days. In contrast for False Alarms, enhanced WCB activity only emerges directly (–2 to

0 days) prior to blocking onset and WCB outflow occurs farther to the west over eastern Greenland and Iceland missing enhanced WCB outflow over Europe, which is evident in ERA-Interim and the Hits forecasts. This shows that the model has an additional potentially erroneous pathway into EuBL that is not found in reanalysis.

We further find a precursor Rossby wave packet emerging from the North Pacific region prior to successful EuBL onset predictions. The downstream development of this Rossby wave pattern goes along with enhanced WCB activity over the North Pacific region up to 10 days prior to EuBL onset. The Rossby wave packet propagates downstream enhancing WCB activity first over eastern North America and later over the central North Atlantic. These upstream precursors are remarkably similar in ERA-Interim and successful reforecasts (Hits) but missing for erroneous EuBL forecasts (False Alarms and Misses).

Though the Rossby wave packet emerging from the North Pacific is associated with increased skill over the Atlantic European region (Grazzini & Vitart, 2015), forecast errors related to small-scale processes inside WCBs could affect the Rossby wave pattern and subsequently lead to errors in the prediction of EuBL onsets. Still, the Rossby wave packet seems to represent a window of forecast opportunity for the prediction of EuBL onset into sub-seasonal timescales which likely depends on an accurate representation of WCB activity conditioned on the MJO in the North Pacific region, too (Quinting et al., 2024).

In summary, our results highlight the role of moist dynamic processes for the correct prediction of EuBL onset. On the one hand, a correct representation of WCB activity in the North Atlantic region in the days prior to EuBL onset results in correct EuBL forecasts. On the other hand, a correct representation of a Rossby wave packet emerging from the North Pacific extends correct EuBL forecasts into sub-seasonal lead times. Interestingly, the North Pacific Rossby wave pattern is also amplified by WCB activity, in line with recent findings by Quinting et al. (2024) who highlighted the potential role of WCBs in shaping tropical-extratropical teleconnection patterns. If and how the MJO further affects EuBL onset should be a subject of future work. Our results suggest, that—in line with similar findings by (e.g., Maddison et al., 2019) - improving the representation of processes inside WCBs and of the associated extratropical cyclones in general (Büeler et al., 2024) in NWP models likely yields a better representation of EuBL life cycles, too. However, we also note that there are intrinsic limits of predictability for WCBs which even a perfect model will not be able to overcome.

Acknowledgments

This research was funded by the Helmholtz Association as part of the Young Investigator Group “Sub-seasonal Predictability: Understanding the Role of Diabatic Outflow” (SPREADOUT, Grant VH-NG-1243) and was partially embedded in the subprojects A8 and B8 of the Transregional Collaborative Research Center SFB/TRR 165 “Waves to Weather” (<https://www.wavestoweather.de>) funded by the German Research Foundation (DFG). The work is based on S2S data. S2S is a joint initiative of the World Weather Research Programme (WWRP) and the World Climate Research Programme (WCRP). The original S2S database is hosted at ECMWF as an extension of the TIGGE database. We thank the large-scale dynamics and predictability group at KIT namely Moritz Pickl, Seraphine Hauser, Joshua Dorrington, Fabian Mockert, Annika Oertel, Marisol Osman, and Marta Wentz for many fruitful discussions and ideas for the manuscript. Furthermore, we thank three reviewers and colleagues from ECMWF (Magdalena Alonso Balmaseda, Linus Magnusson, Frédéric Vitart, and Chris Roberts) for their constructive comments on our results. Lastly, we acknowledge the ECMWF and Deutscher Wetterdienst for granting access to the ERA-Interim data set. Open Access funding enabled and organized by Projekt DEAL.

Data Availability Statement

This study uses freely available data from the ECMWF's sub-seasonal reforecasts (Vitart et al., 2017) and ERA-Interim reanalysis (Dee et al., 2011b), as well as warm conveyor belts calculated with the newly developed ELIAS2.0 metric (Quinting & Grams, 2022b).

References

- Altenhoff, A. M., Martius, O., Croci-Maspoli, M., Schwierz, C., & Davies, H. C. (2008). Linkage of atmospheric blocks and synoptic-scale Rossby waves: A climatological analysis. *Tellus*, *60*(5), 1053–1063. <https://doi.org/10.1111/j.1600-0870.2008.00354.x>
- Anstey, J. A., Davini, P., Gray, L. J., Woollings, T. J., Butchart, N., Cagnazzo, C., et al. (2013). Multi-model analysis of Northern Hemisphere winter blocking: Model biases and the role of resolution. *Journal of Geophysical Research: Atmospheres*, *118*(10), 3956–3971. <https://doi.org/10.1002/jgrd.50231>
- Berggren, R., Bolin, B., & Rossby, C.-G. (1949). An aerological study of zonal motion, its perturbations and break-down. *Tellus*, *1*(2), 14–37. <https://doi.org/10.3402/tellusa.v1i2.8501>
- Berman, J. D., & Torn, R. D. (2019). The impact of initial condition and warm conveyor belt forecast uncertainty on variability in the downstream waveguide in an ECWMF case study. *Monthly Weather Review*, *147*(11), 4071–4089. <https://doi.org/10.1175/mwr-d-18-0333.1>
- Bloomfield, H. C., Brayshaw, D. J., Gonzalez, P. L., & Charlton-Perez, A. (2021). Pattern-based conditioning enhances sub-seasonal prediction skill of European national energy variables. *Meteorological Applications*, *28*(4), e2018. <https://doi.org/10.1002/met.2018>
- Buehler, T., Raible, C. C., & Stocker, T. F. (2011). The relationship of winter season North Atlantic blocking frequencies to extreme cold or dry spells in the ERA-40. *Tellus A: Dynamic Meteorology and Oceanography*, *63*(2), 174–187. <https://doi.org/10.3402/tellusa.v63i2.15797>
- Büeler, D., Ferranti, L., Magnusson, L., Quinting, J. F., & Grams, C. M. (2021). Year-round sub-seasonal forecast skill for Atlantic-European weather regimes. *Quarterly Journal of the Royal Meteorological Society*, *147*(741), 4283–4309. <https://doi.org/10.1002/qj.4178>
- Büeler, D., Sprenger, M., & Wernli, H. (2024). Northern Hemisphere extratropical cyclone biases in ECMWF subseasonal forecasts. *Quarterly Journal of the Royal Meteorological Society*, *150*(759), 1096–1123. <https://doi.org/10.1002/qj.4638>
- Charney, J. G., & DeVore, J. G. (1979). Multiple flow equilibria in the atmosphere and blocking. *Journal of the Atmospheric Sciences*, *36*(7), 1205–1216. [https://doi.org/10.1175/1520-0469\(1979\)036<1205:mfeita>2.0.co;2](https://doi.org/10.1175/1520-0469(1979)036<1205:mfeita>2.0.co;2)
- Colucci, S. J. (1985). Explosive cyclogenesis and large-scale circulation changes: Implications for atmospheric blocking. *Journal of the Atmospheric Sciences*, *42*(24), 2701–2717. [https://doi.org/10.1175/1520-0469\(1985\)042<2701:ecalsc>2.0.co;2](https://doi.org/10.1175/1520-0469(1985)042<2701:ecalsc>2.0.co;2)
- d’Andrea, F., Tibaldi, S., Blackburn, M., Boer, G., Déqué, M., Dix, M., et al. (1998). Northern Hemisphere general circulation models in the period 1979–1988. *Climate Dynamics*, *14*(6), 385–407. <https://doi.org/10.1007/s003820050230>

- Davini, P., Corti, S., D'Andrea, F., Rivière, G., & von Hardenberg, J. (2017). Improved winter European atmospheric blocking frequencies in high-resolution global climate simulations. *Journal of Advances in Modeling Earth Systems*, 9(7), 2615–2634. <https://doi.org/10.1002/2017ms001082>
- Dawson, A., Palmer, T., & Corti, S. (2012). Simulating regime structures in weather and climate prediction models. *Geophysical Research Letters*, 39(21). <https://doi.org/10.1029/2012gl053284>
- Dee, D. P., Uppala, S. M., Simmons, A., Berrisford, P., Poli, P., Kobayashi, S., et al. (2011a). The ERA-Interim reanalysis: Configuration and performance of the data assimilation system. *Quarterly Journal of the Royal Meteorological Society*, 137(656), 553–597. <https://doi.org/10.1002/qj.828>
- Dee, D. P., Uppala, S. M., Simmons, A., Berrisford, P., Poli, P., Kobayashi, S., et al. (2011b). The ERA-Interim reanalysis: Configuration and performance of the data assimilation system [Dataset]. ECMWF. Retrieved from <https://www.ecmwf.int/en/forecasts/dataset/ecmwf-reanalysis-interim>
- Dole, R. M. (1986). The life cycles of persistent anomalies and blocking over the North Pacific. In *Advances in geophysics* (Vol. 29, pp. 31–69). Elsevier.
- Faranda, D., Masato, G., Moloney, N., Sato, Y., Daviaud, F., Dubrulle, B., & Yiou, P. (2016). The switching between zonal and blocked mid-latitude atmospheric circulation: A dynamical system perspective. *Climate Dynamics*, 47(5), 1587–1599. <https://doi.org/10.1007/s00382-015-2921-6>
- Ferranti, L., Corti, S., & Janousek, M. (2015). Flow-dependent verification of the ECMWF ensemble over the Euro-Atlantic sector. *Quarterly Journal of the Royal Meteorological Society*, 141(688), 916–924. <https://doi.org/10.1002/qj.2411>
- Ferranti, L., Magnusson, L., Vitart, F., & Richardson, D. S. (2018). How far in advance can we predict changes in large-scale flow leading to severe cold conditions over Europe? *Quarterly Journal of the Royal Meteorological Society*, 144(715), 1788–1802. <https://doi.org/10.1002/qj.3341>
- Ferro, C. (2014). Fair scores for ensemble forecasts. *Quarterly Journal of the Royal Meteorological Society*, 140(683), 1917–1923. <https://doi.org/10.1002/qj.2270>
- Grams, C. M., & Archambault, H. M. (2016). The key role of diabatic outflow in amplifying the midlatitude flow: A representative case study of weather systems surrounding western North Pacific extratropical transition. *Monthly Weather Review*, 144(10), 3847–3869. <https://doi.org/10.1175/mwr-d-15-0419.1>
- Grams, C. M., Beerli, R., Pfenninger, S., Staffell, I., & Wernli, H. (2017). Balancing Europe's wind-power output through spatial deployment informed by weather regimes. *Nature Climate Change*, 7(8), 557–562. <https://doi.org/10.1038/nclimate3338>
- Grams, C. M., Magnusson, L., & Madonna, E. (2018). An atmospheric dynamics perspective on the amplification and propagation of forecast error in numerical weather prediction models: A case study. *Quarterly Journal of the Royal Meteorological Society*, 144(717), 2577–2591. <https://doi.org/10.1002/qj.3353>
- Grams, C. M., Wernli, H., Böttcher, M., Čampa, J., Corsmeier, U., Jones, S. C., et al. (2011). The key role of diabatic processes in modifying the upper-tropospheric wave guide: A North Atlantic case-study. *Quarterly Journal of the Royal Meteorological Society*, 137(661), 2174–2193. <https://doi.org/10.1002/qj.891>
- Grazzini, F., & Vitart, F. (2015). Atmospheric predictability and Rossby wave packets. *Quarterly Journal of the Royal Meteorological Society*, 141(692), 2793–2802. <https://doi.org/10.1002/qj.2564>
- Hauser, S. (2023). A novel quasi-Lagrangian perspective on the potential vorticity dynamics of blocked weather regime life cycles in the North Atlantic-European region (Doctoral dissertation, Karlsruhe Institut für Technologie (KIT)). <https://doi.org/10.5445/IR/1000162808>
- Hauser, S., Teubler, F., Riemer, M., Knippertz, P., & Grams, C. M. (2023a). Life cycle dynamics of Greenland blocking from a potential vorticity perspective. *EGU Sphere*, 1–37. <https://doi.org/10.5194/egusphere-2023-2945>
- Hauser, S., Teubler, F., Riemer, M., Knippertz, P., & Grams, C. M. (2023b). Towards a holistic understanding of blocked regime dynamics through a combination of complementary diagnostic perspectives. *Weather and Climate Dynamics*, 4(2), 399–425. <https://doi.org/10.5194/wcd-4-399-2023>
- Hochman, A., Messori, G., Quinting, J. F., Pinto, J. G., & Grams, C. M. (2021). Do Atlantic-European weather regimes physically exist? *Geophysical Research Letters*, 48(20), e2021GL095574. <https://doi.org/10.1029/2021gl095574>
- Hoskins, B. J., & Karoly, D. J. (1981). The steady linear response of a spherical atmosphere to thermal and orographic forcing. *Journal of the Atmospheric Sciences*, 38(6), 1179–1196. [https://doi.org/10.1175/1520-0469\(1981\)038<1179:tslroa>2.0.co;2](https://doi.org/10.1175/1520-0469(1981)038<1179:tslroa>2.0.co;2)
- Jia, X., Yang, S., Song, W., & He, B. (2014). Prediction of wintertime Northern Hemisphere blocking by the NCEP climate forecast system. *Journal of Meteorological Research*, 28(1), 76–90. <https://doi.org/10.1007/s13351-014-3085-8>
- Maddison, J. W., Gray, S. L., Martínez-Alvarado, O., & Williams, K. D. (2019). Upstream cyclone influence on the predictability of block onsets over the Euro-Atlantic region. *Monthly Weather Review*, 147(4), 1277–1296. <https://doi.org/10.1175/MWR-D-18-0226.1>
- Maddison, J. W., Gray, S. L., Martínez-Alvarado, O., & Williams, K. D. (2020). Impact of model upgrades on diabatic processes in extratropical cyclones and downstream forecast evolution. *Quarterly Journal of the Royal Meteorological Society*, 146(728), 1322–1350. <https://doi.org/10.1002/qj.3739>
- Madonna, E., Wernli, H., Joos, H., & Martius, O. (2014). Warm conveyor belts in the ERA-Interim dataset (1979–2010). Part I: Climatology and potential vorticity evolution. *Journal of Climate*, 27(1), 3–26. <https://doi.org/10.1175/jcli-d-12-00720.1>
- Martínez-Alvarado, O., Madonna, E., Gray, S. L., & Joos, H. (2016). A route to systematic error in forecasts of Rossby waves. *Quarterly Journal of the Royal Meteorological Society*, 142(694), 196–210. <https://doi.org/10.1002/qj.2645>
- Masato, G., Woollings, T., & Hoskins, B. (2014). Structure and impact of atmospheric blocking over the Euro-Atlantic region in present-day and future simulations. *Geophysical Research Letters*, 41(3), 1051–1058. <https://doi.org/10.1002/2013gl058570>
- Mastrantonas, N., Magnusson, L., Pappenberger, F., & Matschullat, J. (2022). What do large-scale patterns teach us about extreme precipitation over the Mediterranean at medium- and extended-range forecasts? *Quarterly Journal of the Royal Meteorological Society*, 148(743), 875–890. <https://doi.org/10.1002/qj.4236>
- Michel, C., & Rivière, G. (2011). The link between Rossby wave breakings and weather regime transitions. *Journal of the Atmospheric Sciences*, 68(8), 1730–1748. <https://doi.org/10.1175/2011jas3635.1>
- Michel, C., Rivière, G., Terray, L., & Joly, B. (2012). The dynamical link between surface cyclones, upper-tropospheric Rossby wave breaking and the life cycle of the Scandinavian blocking. *Geophysical Research Letters*, 39(10). <https://doi.org/10.1029/2012GL051682>
- Michelangeli, P.-A., Vautard, R., & Legras, B. (1995). Weather regimes: Recurrence and quasi stationarity. *Journal of the Atmospheric Sciences*, 52(8), 1237–1256. [https://doi.org/10.1175/1520-0469\(1995\)052<1237:wrraqs>2.0.co;2](https://doi.org/10.1175/1520-0469(1995)052<1237:wrraqs>2.0.co;2)
- Mohr, S., Wandel, J., Lenggenhager, S., & Martius, O. (2019). Relationship between atmospheric blocking and warm-season thunderstorms over western and central Europe. *Quarterly Journal of the Royal Meteorological Society*, 145(724), 3040–3056. <https://doi.org/10.1002/qj.3603>

- Nakamura, N., & Huang, C. S. (2018). Atmospheric blocking as a traffic jam in the jet stream. *Science*, *361*(6397), 42–47. <https://doi.org/10.1126/science.aat0721>
- Oertel, A., Boettcher, M., Joos, H., Sprenger, M., & Wernli, H. (2020). Potential vorticity structure of embedded convection in a warm conveyor belt and its relevance for large-scale dynamics. *Weather and Climate Dynamics*, *1*(1), 127–153. <https://doi.org/10.5194/wcd-1-127-2020>
- Oertel, A., Miltenberger, A. K., Grams, C. M., & Hoose, C. (2023). Interaction of microphysics and dynamics in a warm conveyor belt simulated with the ICOSahedral Nonhydrostatic (ICON) model. *Atmospheric Chemistry and Physics*, *23*(15), 8553–8581. <https://doi.org/10.5194/acp-23-8553-2023>
- Oertel, A., Pickl, M., Quinting, J. F., Hauser, S., Wandel, J., Magnusson, L., et al. (2023). Everything hits at once: How remote rainfall matters for the prediction of the 2021 North American heat wave. *Geophysical Research Letters*, *50*(3), e2022GL100958. <https://doi.org/10.1029/2022GL100958>
- Osman, M., Beerli, R., Büeler, D., & Grams, C. M. (2023). Multi-model assessment of sub-seasonal predictive skill for year-round Atlantic-European weather regimes. *Quarterly Journal of the Royal Meteorological Society*, *149*(755), 2386–2408. <https://doi.org/10.1002/qj.4512>
- Pfahl, S., Schwierz, C., Croci-Maspoli, M., Grams, C. M., & Wernli, H. (2015). Importance of latent heat release in ascending air streams for atmospheric blocking. *Nature Geoscience*, *8*(8), 610–614. <https://doi.org/10.1038/ngeo2487>
- Pfahl, S., & Wernli, H. (2012). Quantifying the relevance of atmospheric blocking for co-located temperature extremes in the Northern Hemisphere on (sub-) daily time scales. *Geophysical Research Letters*, *39*(12). <https://doi.org/10.1029/2012gl052261>
- Pickl, M., Quinting, J. F., & Grams, C. M. (2023). Warm conveyor belts as amplifiers of forecast uncertainty. *Quarterly Journal of the Royal Meteorological Society*, *149*(756), 3064–3085. <https://doi.org/10.1002/qj.4546>
- Pomroy, H. R., & Thorpe, A. J. (2000). The evolution and dynamical role of reduced upper-tropospheric potential vorticity in intensive observing period one of FASTEX. *Monthly Weather Review*, *128*(6), 1817–1834. [https://doi.org/10.1175/1520-0493\(2000\)128<1817:teadro>2.0.co;2](https://doi.org/10.1175/1520-0493(2000)128<1817:teadro>2.0.co;2)
- Quinting, J. F., & Grams, C. M. (2022a). Eulerian Identification of ascending AirStreams (ELIAS 2.0) in numerical weather prediction and climate models. Part I: Development of deep learning model. *Geoscientific Model Development*, *15*(2), 715–730. <https://doi.org/10.5194/gmd-15-715-2022>
- Quinting, J. F., & Grams, C. M. (2022b). Eulerian Identification of ascending AirStreams (ELIAS 2.0) in numerical weather prediction and climate models [Software]. Part I: Development of deep learning model. Retrieved from https://git.scc.kit.edu/nk2448/wcbmetric_v2/
- Quinting, J. F., Grams, C. M., Chang, E. K.-M., Pfahl, S., & Wernli, H. (2024). Warm conveyor belt activity over the Pacific: Modulation by the Madden-Julian Oscillation and impact on tropical-extratropical teleconnections. *Weather and Climate Dynamics*, *5*(1), 65–85. <https://doi.org/10.5194/wcd-5-65-2024>
- Quinting, J. F., & Vitart, F. (2019). Representation of synoptic-scale Rossby wave packets and blocking in the S2S prediction project database. *Geophysical Research Letters*, *46*(2), 1070–1078. <https://doi.org/10.1029/2018gl081381>
- Rex, D. F. (1950). Blocking action in the middle troposphere and its effect upon regional climate. *Tellus*, *2*(4), 275–301. <https://doi.org/10.1111/j.2153-3490.1950.tb00331.x>
- Riboldi, J., Grams, C. M., Riemer, M., & Archambault, H. M. (2019). A phase locking perspective on Rossby wave amplification and atmospheric blocking downstream of recurring western North Pacific Tropical Cyclones. *Monthly Weather Review*, *147*(2), 567–589. <https://doi.org/10.1175/MWR-D-18-0271.1>
- Rodwell, M. J., Magnusson, L., Bauer, P., Bechtold, P., Bonavita, M., Cardinali, C., et al. (2013). Characteristics of occasional poor medium-range weather forecasts for Europe. *Bulletin of the American Meteorological Society*, *94*(9), 1393–1405. <https://doi.org/10.1175/bams-d-12-00099.1>
- Shutts, G. (1983). The propagation of eddies in diffluent jetstreams: Eddy vorticity forcing of 'blocking' flow fields. *Quarterly Journal of the Royal Meteorological Society*, *109*(462), 737–761. <https://doi.org/10.1002/qj.49710946204>
- Steinfeld, D., Boettcher, M., Forbes, R., & Pfahl, S. (2020). The sensitivity of atmospheric blocking to upstream latent heating – Numerical experiments. *Weather and Climate Dynamics*, *1*(2), 405–426. <https://doi.org/10.5194/wcd-1-405-2020>
- Steinfeld, D., & Pfahl, S. (2019). The role of latent heating in atmospheric blocking dynamics: A global climatology. *Climate Dynamics*, *53*(9), 6159–6180. <https://doi.org/10.1007/s00382-019-04919-6>
- Teubler, F., & Riemer, M. (2021). Potential-vorticity dynamics of troughs and ridges within rossby wave packets during a 40-year reanalysis period. *Weather and Climate Dynamics*, *2*(3), 535–559. <https://doi.org/10.5194/wcd-2-535-2021>
- Teubler, F., Riemer, M., Polster, C., Grams, C. M., Hauser, S., & Wirth, V. (2023). Similarity and variability of blocked weather-regime dynamics in the Atlantic–European region. *Weather and Climate Dynamics*, *4*(2), 265–285. <https://doi.org/10.5194/wcd-4-265-2023>
- Vautard, R. (1990). Multiple weather regimes over the North Atlantic: Analysis of precursors and successors. *Monthly Weather Review*, *118*(10), 2056–2081. [https://doi.org/10.1175/1520-0493\(1990\)118<2056:mwrotn>2.0.co;2](https://doi.org/10.1175/1520-0493(1990)118<2056:mwrotn>2.0.co;2)
- Vitart, F. (2017). Madden—Julian Oscillation prediction and teleconnections in the S2S database. *Quarterly Journal of the Royal Meteorological Society*, *143*(706), 2210–2220. <https://doi.org/10.1002/qj.3079>
- Vitart, F., Ardilouze, C., Bonet, A., Brookshaw, A., Chen, M., Codorean, C., et al. (2017). The subseasonal to seasonal (S2S) prediction project database [Dataset]. *ECMWF*. Retrieved from <https://apps.ecmwf.int/datasets/data/s2s/>
- Wandel, J., Quinting, J. F., & Grams, C. M. (2021). Toward a systematic evaluation of warm conveyor belts in numerical weather prediction and climate models. Part II: Verification of operational reforecasts. *Journal of the Atmospheric Sciences*, *78*(12), 3965–3982. <https://doi.org/10.1175/JAS-D-20-0385.1>
- Wernli, H. (1997). A Lagrangian-based analysis of extratropical cyclones. II: A detailed case-study. *Quarterly Journal of the Royal Meteorological Society*, *123*(542), 1677–1706. <https://doi.org/10.1002/qj.49712354211>
- Wernli, H., & Davies, H. C. (1997). A Lagrangian-based analysis of extratropical cyclones. I: The method and some applications. *Quarterly Journal of the Royal Meteorological Society*, *123*(538), 467–489. <https://doi.org/10.1256/smsqj.53810>
- Yamazaki, A., & Itoh, H. (2013). Vortex–vortex interactions for the maintenance of blocking. Part I: The selective absorption mechanism and a case study. *Journal of the Atmospheric Sciences*, *70*(3), 725–742. <https://doi.org/10.1175/jas-d-11-0295.1>